Volume 7, Number 7
1004-423X/98/07070529-12

ACTA PHYSICA SINICA
(Overseas Edition)

July, 1998
© 1998 Chin. Phys. Soc.

EXCHANGE COUPLING BETWEEN TWO MAGNETIZED LAYERS IN A METAL

Wang Shao-feng(王少峰)

Center of Physics and Mathematics, Xi'an Jiaotong University, Xi'an 710049,China

Wang Zhong-cheng(汪仲诚) and Zou Shi-chang(邹世昌)

State Key Laboratory of Functional Materials for Informatics,

Shanghai Institute of Metallurgy, Academia Sinica, Shanghai 200050, China

(Received 26 August 1997; revised manuscript received 29 December 1997)

The exchange coupling energy for two magnetized monolayers embedded symmetrically in a metal and polarized in an arbitrary direction has been investigated in contact interaction approximation. Since the model can be solved exactly in particular for free-electron case, the coupling energy contributed from both extended state electrons and bound state electrons is calculated rigorously. For weak interaction, it is found that the leading term in the power-series expansion of density of states can give a correct coupling energy compared with rigorous one while extended state electrons give a much larger coupling energy. Furthermore, the relevant problems such as phase shift, 90° coupling and lattice effects have been discussed; an asymptotic expression of the interlayer coupling has been derived in a different way and used to calculate the exchange energy between magnetic layers in copper with Fermi surface obtained from de Haas-van Alphen effect.

PACC: 7570

I. INTRODUCTION

Since the discovery of antiferromagnetic exchange coupling[1] and the subsequent discovery of coupling oscillation[2] in Fe/Cr/Fe magnetic multilayer structure and many other similar structures, the exchange coupling between magnetic layers separated by a nonmagnetic spacer has been a subject of intense research. Although much progress has been made in theoretical and experimental researches of this field, there still some problems remain to be clarified. For instance, the theoretically calculated coupling strength is usually much larger than that obtained in experiments.

The exchange coupling energy (ECE) between magnetic monolayers was first studied by Bruno *et al.*[3] in the context of RKKY theory. Most of the oscillatory characteristics can be predicted by their model. On the other hand, ECE is also studied in the frame of spin-dependent quantum well model[4,5] for magnetic sandwich structure. In this paper, within contact interaction approximation, ECE between two magnetic monolayers embedded in a metal is investigated under the assumption that spin-flip can be neglected due to strong correlated-interaction among the spins in a layer. Similar model has been studied by several authors and used to explain the elementary features observed in magnetic mutilayer structure.[6−9] Here, the previous model has been improved by taking into account the

difference between the host atom and doping atom and allowing the magnetic layers polarized in an arbitrary direction.

The model can be solved unperturbatively. In particular, the change in density of states (DOS) is obtained exactly; and ECE, including the contribution from bound state electrons as well as extended state electrons, is calculated accurately for free-electron case. It is found that the contribution from bound state electrons is comparable with that from extended state electrons. However, these two contributions cancel each other and result in a much smaller summation. For weak interaction, it is interesting to note that the leading term in the expansion series of DOS can give a desirable result although the bound electron is omitted in the approximation. This result is instructive for *ab initio* numerical calculation, which frequently give a much larger ECE compared with experimental data. For a first-principle calculation of ECE, it seems more convenient to use the leading term approximation rather than the exact expression of DOS. Furthermore, it is found that exchange split in a magnetic layer mainly dominates the magnitude of ECE while conduction band position relative to that of the host metal has a major influence on the oscillatory phase. And a normalized ECE for Cu(111) is evaluated by using the Fermi surface obtained from de Haas-van Alphen effect.[10]

II. MODEL

We consider two parallel monolayers embedded in a nonmagnetic metal. Each layer is a plane consisting of magnetic atoms located on the atomic position $\boldsymbol{R}$ of the host metal. The extra interaction between a conduction electron with spin $\boldsymbol{s}$ at position $\boldsymbol{r}$ and a localized magnetic atom with spin $\boldsymbol{S}$ at the position $\boldsymbol{R}$ is approximated by a contact potential

$$v_{ex} = [\zeta + J\boldsymbol{s}\cdot\boldsymbol{S}(\boldsymbol{R})]\delta(\boldsymbol{r}-\boldsymbol{R}) \ , \tag{1}$$

where J is the exchange interaction constant, ζ is introduced to describe the distinction between magnetic atom and host atom in addition to spin difference. The interaction Hamiltonian for an electron coupled to the layers is obtained by summing over the localized spins

$$H_{\rm I} = \sum_{\boldsymbol{R}_\parallel}\{[\zeta + J\boldsymbol{s}\cdot\boldsymbol{S}(\boldsymbol{R}_\parallel)]\delta(\boldsymbol{r}-\boldsymbol{R}_\parallel) + [\zeta + J\boldsymbol{s}\cdot\boldsymbol{S}(\boldsymbol{R}_\parallel+\boldsymbol{R}^0)]\delta(\boldsymbol{r}-\boldsymbol{R}_\parallel-\boldsymbol{R}^0)\} \ , \tag{2}$$

where $\boldsymbol{R}_\parallel$ is a lattice vector on the plane, $\boldsymbol{R}^0 = \boldsymbol{R}^0_\parallel + d\hat{\boldsymbol{z}}$ is the position vector of the second layer relative to the first layer; the distance between the two layers is $d = (\delta N + 1)d_0$, where d_0 is the spacing between atomic planes and δN is the number of atomic planes of the spacer. Following Ref.[8], the spins in a magnetic layer are generally correlated so strongly that the localized spins $\boldsymbol{S}(\boldsymbol{R})$ can be approximately regarded as only dependent on the layers and can be taken out from the summation.

$$\begin{aligned} H_{\rm I} &= [\zeta + J\boldsymbol{s}\cdot\boldsymbol{S}(\boldsymbol{R}_\parallel)]\sum_{\boldsymbol{R}_\parallel}\delta(\boldsymbol{r}-\boldsymbol{R}_\parallel) + [\zeta + J\boldsymbol{s}\cdot\boldsymbol{S}(\boldsymbol{R}_\parallel+\boldsymbol{R}^0)]\sum_{\boldsymbol{R}_\parallel}\delta(\boldsymbol{r}-\boldsymbol{R}_\parallel-\boldsymbol{R}^0) \\ &= \alpha_1\sum_{\boldsymbol{R}_\parallel}\delta(\boldsymbol{r}-\boldsymbol{R}_\parallel) + \alpha_2\sum_{\boldsymbol{R}_\parallel}\delta(\boldsymbol{r}-\boldsymbol{R}_\parallel-\boldsymbol{R}^0) \ , \end{aligned} \tag{3}$$

where $\boldsymbol{S}_1$ ($\boldsymbol{S}_2$) is the representative spin of the layers, and

$$\alpha_i = \zeta + Js \cdot \boldsymbol{S}_i \qquad i = 1, 2. \tag{4}$$

Equation(3) represents a spin-dependent potential, which is the basis of the following discussion. This potential is closely related with the energy band structure of a magnetic layer. Actually, exchange interaction constant J can be considered as describing exchange split of the energy band of a magnetic layer; and ζ describes conduction-band shift of the magnetic layer relative to that of the host metal. A perturbative spin-dependent potential will introduce an additional energy to the conduction electron system. This part of energy which is to be calculated depends on the alignments of the magnetized layers and dominates the kind of alignment which will appear in practice.

It is convenient to choose the spin orientation (magnetization) of one layer to be $\boldsymbol{z}$ axis of the spin space, and write α_i as

$$\alpha_1 = \zeta + JsS\ \sigma_z, \qquad \alpha_2 = \zeta + JsS\ \boldsymbol{\sigma} \cdot \boldsymbol{n},$$

where S and s are, respectively, the spin quantum numbers of a magnetic atom and an electron, $\boldsymbol{\sigma} = (\sigma_x, \sigma_y, \sigma_z)$ are Pauli matrixes, unit vector $\boldsymbol{n} = -\sin\theta\hat{\boldsymbol{y}} + \cos\theta\hat{\boldsymbol{z}}$ is the spin orientation of another layer, and θ is the angle between the magnetizations of two layers.

III. FREE-ELECTRON APPROXIMATION

Generally, the fundamental physics underlying a phenomenon can be illustrated simply by a free-electron model. To make the treatment consistent with our statement, it is reasonable to assume that magnetic atoms in a magnetized layer distribute continuously and uniformly. The summation over $\boldsymbol{R}_\parallel$ can be replaced by integration

$$\sum_{\boldsymbol{R}_\parallel} \longrightarrow \int \frac{\mathrm{d}\boldsymbol{R}_\parallel}{\tau}\ ,$$

where τ is the area of a two-dimensional primitive cell of a magnetized layer. Now, Eq.(3) can be written as

$$H_{\mathrm{I}} = \sum_{i=1}^{2} \frac{\alpha_i}{\tau} \delta(z - z_i)\ , \tag{5}$$

where z_1 and z_2 are the position coordinates of the layers. For simplicity, τ will be absorbed by α_i in this section through redefining the interaction constant $\zeta/\tau \to \zeta$ and $J/\tau \to J$. In the representation of free-electron with a bound boundary condition

$$|n\rangle = \sqrt{\frac{2}{L}} \sin\frac{n\pi z}{L}, \qquad \varepsilon_n = \frac{\hbar^2\pi^2 n^2}{2mL^2} \qquad n = 1, 2, 3....$$

it is easy to see that one-dimensional 2×2 Green's function g satisfies the following matrix equation:

$$(\omega - \varepsilon_n) g(n, m) - \sum_l H^{\mathrm{I}}(n, l)\, g(l, m) = \delta_{nm}, \tag{6}$$

$$H^{\mathrm{I}}(n,l) = \langle n|H^I|l\rangle = \frac{2}{L}\sum_{i=1}^{2}\alpha_i \sin\left(\frac{n\pi z_i}{L}\right)\sin\left(\frac{l\pi z_i}{L}\right), \tag{7}$$

where ω is the energy with an infinitesimal imaginary part $\omega = E+\mathrm{i}\eta\,(\eta>0)$. By introducing matrixes

$$T_i = \alpha_i \sum_l \sin\left(\frac{l\pi z_i}{L}\right) g(l,m) \qquad i=1,2\ ,$$

the Green's function can be written as

$$g(n,m) = \frac{1}{\omega-\varepsilon_n}\left[\delta_{nm} + \frac{2}{L}\sum_{i=1}^{2}\sin\left(\frac{n\pi z_i}{L}\right) T_i\right]. \tag{8}$$

Following the way presented in Ref.[8], we find

$$\begin{aligned} MT_1 &= C_2 D + C_1(\alpha_2^{-1} - F_2),\\ M^+T_2 &= C_1 D + C_2(\alpha_1^{-1} - F_1), \end{aligned}$$

where

$$C_i = \frac{\sin(m\pi z_i/L)}{\omega-\varepsilon_m} \qquad i=1,2; \qquad M = \left[(\alpha_2^{-1}-F_2)(\alpha_1^{-1}-F_1) - D^2\right]\ ,$$

and functions F_i $(i=1,2)$ and D are defined by

$$\begin{aligned} F_i &= \frac{2}{L}\sum_{n=1}^{\infty}\frac{\sin^2(n\pi z_i/L)}{\omega-\varepsilon_n} \qquad i=1,2,\\ D &= \frac{2}{L}\sum_{n=1}^{\infty}\frac{\sin(n\pi z_1/L)\sin(n\pi z_2/L)}{\omega-\varepsilon_n}. \end{aligned}$$

In order to get an analytical expression, it is useful to expand 2×2 matrix M by using Pauli matrixes $\boldsymbol{\sigma}$

$$M = p_0 + \boldsymbol{p}\cdot\boldsymbol{\sigma}\ , \tag{9}$$

where p_0 and $\boldsymbol{p} = (p_x, p_y, p_z)$ are given by

$$\begin{aligned} p_0 &= \left(F_1+\frac{\gamma}{\nu}\right)\left(F_2+\frac{\gamma}{\nu}\right) - D^2 - \frac{\cos\theta}{\nu}\ ,\\ p_x &= -\frac{\mathrm{i}\sin\theta}{\nu^2}\ , \qquad p_y = -\left(F_1+\frac{\gamma}{\nu}\right)\frac{\sin\theta}{\nu}\ ,\\ p_z &= -\left(F_1+\frac{\gamma}{\nu}\right)\frac{\cos\theta}{\nu} - \frac{1}{\nu}\left(F_2+\frac{\gamma}{\nu}\right)\ , \end{aligned}$$

with

$$\gamma = \frac{\zeta}{JsS} \qquad \text{and} \qquad \nu = JsS\left[1-\left(\frac{\zeta}{JsS}\right)^2\right]\ . \tag{10}$$

Apparently, we have

$$M^{-1} = \frac{p_0 - \boldsymbol{p}\cdot\boldsymbol{\sigma}}{p_0^2 - p^2}\ .$$

The functions F_i, and D can be obtained exactly for arbitrary L

$$F_i = \frac{\pi}{\varepsilon_0 \kappa a} \frac{1}{\sin(2\pi\kappa L/a)} \left[\cos\left(\frac{2\pi\kappa L}{a}\right) - \cos(2z_i - L)\frac{2\pi\kappa}{a} \right] , \tag{11}$$

$$D = \frac{\pi}{\varepsilon_0 \kappa a} \frac{1}{\sin(2\pi\kappa L/a)} \left[\cos(L - z_2 + z_1)\frac{2\pi\kappa}{a} - \cos(L - z_2 - z_1)\frac{2\pi\kappa}{a} \right] , \tag{12}$$

with

$$\kappa = \sqrt{\frac{\omega}{\varepsilon_0}} , \qquad \varepsilon_0 = \frac{\hbar^2}{2m}\left(\frac{2\pi}{a}\right)^2 ,$$

where a is introduced as a characteristic length and can be chosen to be either the lattice constant or the Fermi wavelength λ_{F}. In the numerical calculations given below, we choose $a = \lambda_{\mathrm{F}}$ and $\varepsilon_0 = E_{\mathrm{F}}$ (Fermi energy). Equations (11) and (12) are useful for investigating quantum size effects when L is comparable to d. The problem will be complicated tremendously if the quantum size effects are not negligible. In what follows we restrict ourselves to the limit $L \longrightarrow \infty$. In this case, F and D may be simplified as

$$F = -\frac{\mathrm{i}\pi}{\varepsilon_0 a \kappa} \qquad \text{and} \qquad D = F\mathrm{e}^{\mathrm{i}2\pi\kappa d/a}. \tag{13}$$

It can be verified directly that the three-dimensional Green's function is given by

$$G(\omega) = g(\omega - \varepsilon_{\parallel})\delta_{\boldsymbol{k}_{\parallel}\boldsymbol{k}'_{\parallel}} , \qquad \varepsilon_{\parallel} = \frac{\hbar^2 \boldsymbol{k}_{\parallel}^2}{2m} ,$$

and the trace $\mathrm{Tr}G$ of the Green's function can be written as

$$\mathrm{Tr}G = \mathrm{Tr}G_0 + \rho_{\parallel} \ln \Delta(\omega) , \tag{14}$$

where $\rho_{\parallel} = m/(2\pi\hbar^2)$ is the two-dimensional DOS in unit area, Δ is defined by

$$\Delta = 1 + [(\gamma + \nu F)^2 - \nu^2 D^2]^2 - 2[(\gamma + \nu F)^2 + \nu^2 D^2 \cos\theta] . \tag{15}$$

The dependence of Δ on the angle θ can be expressed as

$$\Delta(\theta) = \Delta_0 + 4\nu^2 D^2 \sin^2\left(\frac{\theta}{2}\right) , \tag{16}$$

where $\Delta_0 = \Delta(\theta = 0)$ corresponds to the ferromagnetical configuration. And Δ also can be split into a product $\Delta = \Delta_+\Delta_-$, where Δ_+ and Δ_- are, respectively, related to the two spin eigenstates which depend on angle θ

$$\Delta_{\pm} = 1 - \gamma^2 + \left(\frac{\tilde{\nu}}{\kappa}\right)^2 (1 - \mathrm{e}^{\mathrm{i}4\pi\kappa d/a}) + \mathrm{i}\frac{2\tilde{\nu}}{\kappa}\left[\gamma \pm \cos\left(\frac{\theta}{2}\right)\mathrm{e}^{\mathrm{i}2\pi\kappa d/a}\right] ,$$

where dimensionless parameter $\tilde{\nu}$ is defined as

$$\tilde{\nu} = \frac{\pi\nu}{\varepsilon_0 a} = \alpha(1 - \gamma^2), \quad \alpha = \frac{\pi J s S}{\varepsilon_0 a} .$$

The DOS is given by

$$\rho(E) = -\frac{1}{\pi}\mathrm{Im}\mathrm{Tr}G(E+i\eta)|_{\eta\to 0^+} = \rho_0(E) + \tilde{\rho}(E)\ , \tag{17}$$

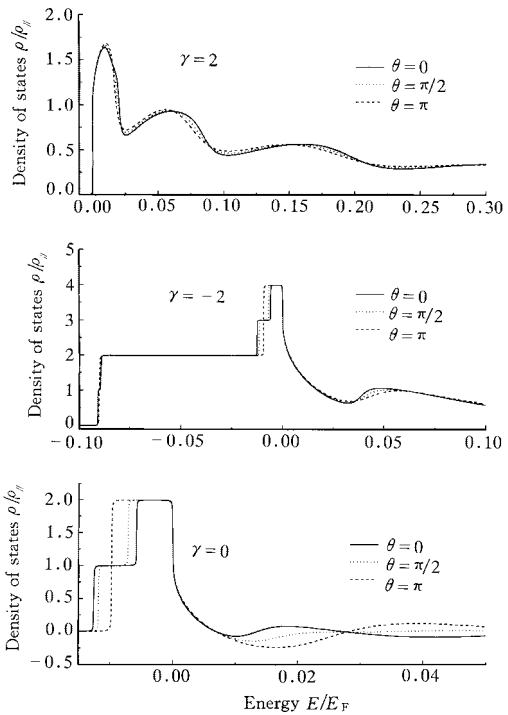

Fig.1. The change in DOS due to the presence of magnetized layers, $d = 3\lambda_F$ and $\alpha = 0.1$. A bound state with $E < 0$ appears when DOS has a unit jump.

where $\rho_0(E)$ is the DOS of the unperturbed conduction electron, $\tilde{\rho}(E)$ is the modification due to the presence of magnetized layers

$$\tilde{\rho}(E) = \rho_\parallel(-\frac{1}{\pi}\mathrm{Im}\ln\Delta)|_{\eta\to 0^+}\ . \tag{18}$$

The $\tilde{\rho}$ given by Eq.(18) is a multi-value function. A physically meaningful one can be selected uniquely by the following two rules: (i) $\tilde{\rho}$ must be continuous when the imaginary part $\eta > 0$ is a very small but nonzero positive number; (ii) $\tilde{\rho}$ must vanish for sufficiently large energy E. In Fig.1, the changes in DOS are shown for some typical magnetic configurations, where θ is the angle between the magnetizations of the layers. The bound state appears at the energy $E < 0$, where DOS has a step jump. For $E > 0$, DOS oscillates with a period determined by the distance d and falls off gradually.

The coupling energy corresponding to a given configuration is obtained by

$$U = \int_{-\infty}^{E_F} (E - E_F)\rho(E)\mathrm{d}E\ . \tag{19}$$

For a given magnetic configuration of the magnetized layers, the ECE can be defined as the difference of the coupling energies compared with ferromagnetic one,

$$W = U|_\theta - U|_{\theta=0} = \int_{-\infty}^{E_F} (E - E_F)\delta\tilde{\rho}(E)\mathrm{d}E\ , \tag{20}$$

$$\delta\tilde{\rho} = \rho_\parallel\left[-\frac{1}{\pi}\mathrm{Im}\ln\left(1 + \frac{4\nu^2 D^2}{\Delta_0}\sin^2\left(\frac{\theta}{2}\right)\right)\right]\ . \tag{21}$$

The stable configuration is given theoretically by minimum energy principle.

From Eqs. (20) and (21), ECE has been calculated numerically and results are shown in Figs. 2–4. As we see from Fig.2, the contribution from bound state electrons is comparable

with that from extended state electrons. But the two contributions counteract each other and result in a much smaller ECE, which oscillates with a period $\lambda_F/2$. The result indicates that one should be careful in calculating the absolute strength of the exchange energy.

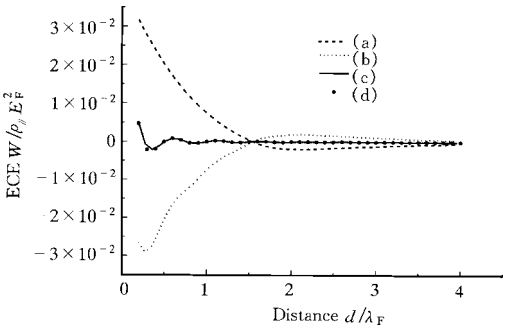

Fig.2. An illustration of the contributions to the ECE separately from extended state electrons and bound state electrons, $\alpha = 0.1$ and $\gamma = 0$. (a) Contribution of bound state, (b) contribution of extended state, (c) total sum which oscillates with the distance, (d) leading term approximation. Each individual contribution is much larger than actual one resulting from summation.

For weak interaction $\nu \ll 1$ and $\gamma \ll 1$, we expand $\delta\tilde{\rho}$ in series of ν, and keep only the leading term in Eq.(20). After integration, we have

$$W = \frac{8\alpha^2\varepsilon_0 E_F \rho_{\parallel}}{\pi(1-\gamma^2)} \sin^2\left(\frac{\theta}{2}\right)\left[-\frac{\pi}{2} + \Phi(2k_F d)\right], \tag{22}$$

$$\Phi(x) = -\mathrm{si}(x) - \frac{\cos x}{x} + \frac{\sin x}{x} \approx \frac{2\sin x}{x^2},$$

where $\mathrm{si}(x)$ is the sine integral function. The constant $\pi/2$ in Eq.(22) which leads to a long-range interaction has been discussed by Kittel[11] and Yafat.[12] Obviously, the bound state dose not incorporate and a singularity at $\kappa = 0$ has been introduced in the leading term approximation. This is the reason for the appearance of $\pi/2$. However, from Fig.2 and Fig.3 (c), it is interesting to note that if the constant $\pi/2$ is omitted, ECE given by Eq.(22) agrees well with the rigorous result. Based on this observation, we propose that instead of using exact DOS, it seems more convenient to calculate ECE with the leading term approximation when a first-principle calculation is undertaken.

The strength of ECE is mainly determined by the magnitude of exchange interaction J. As shown in Fig.3 (c), for weak exchange interaction, the ECE changes a little as γ varies from -10 to 10. For relatively strong exchange interaction, a phase shift appears, for example, for $\alpha = 0.1$, there is nearly a π phase shift when the magnitude of γ changes from 0 to 10 (Fig.3). From Fig.3, we also see that the magnitude of exchange interaction J has little effect on the phase shift. Since ζ is the counterpart of the average shift of the band relative to that of host metal, we can conclude that the strength is mainly dominated by exchange split while the phase shift is mainly set by relative position of the conduction bands.

The dependence of ECE on the angle between the magnetizations of two layers has been investigated numerically for some of fixed distance d. The distance d is chosen to be near the transition point at which magnetic configuration changes from parallel to antiparallel alignment and the quadratic coupling vanishes. The results are shown in Fig.4. Although sometimes extreme points appear near $\theta = \pi/2$, within the calculating accuracy, the minimum position, that corresponds to stable magnetic configuration of the layers, is either at

$\theta = 0$ (parallel alignment) or at $\theta = \pi$ (antiparallel alignment). It can be concluded that no stable non-parallel configuration, in particular the 90° alignment, exists in the model.

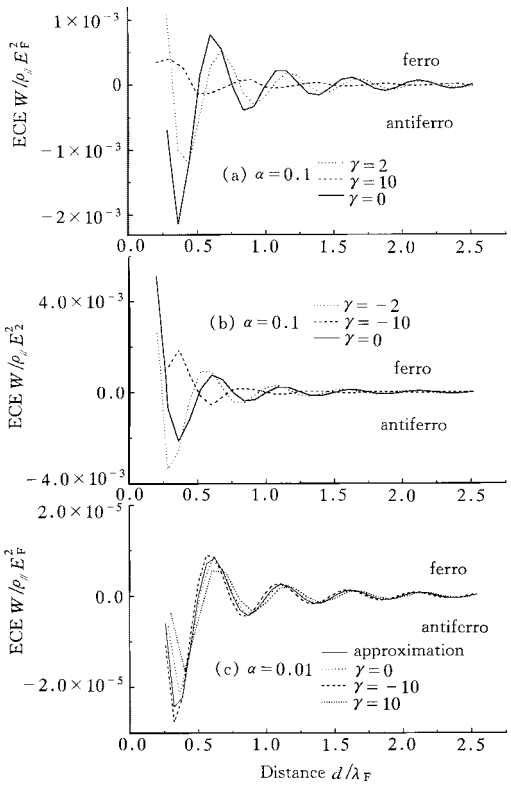

Fig.3. An illustration of the detail dependence of ECE on the spin-dependent potential. The approximation one is given for $\gamma = 0$.

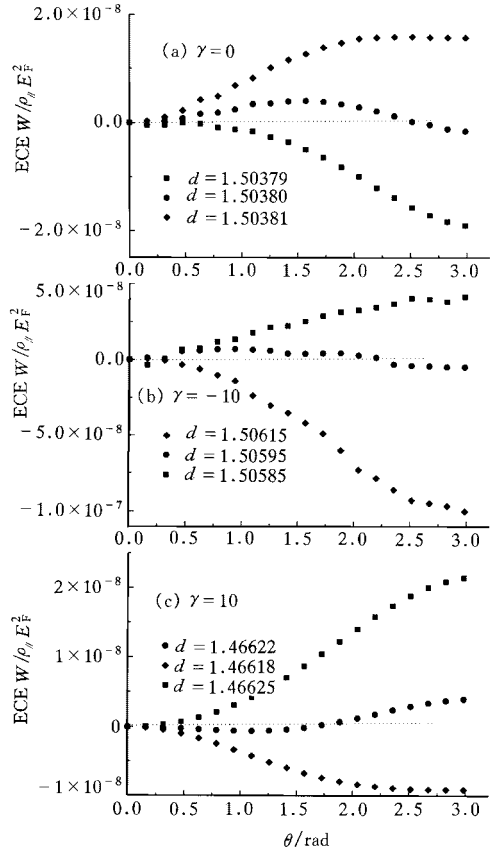

Fig.4. Typical behaviors of ECE versus angle θ near the transition point, $\alpha = 0.1$, θ is the angle between the magnetizations of two layers. Transition from ferromagnetic to antiferromagnetic occurs as distance d changes slightly. Note that the magnitude of ECE is in the order of 10^{-2} at the distance $d \sim 1.5$. Obviously, in a greater accuracy, no 90° alignment appears.

IV. LATTICE EFFECTS

The above discussion can be straightforwardly generalized to include lattice effects that mainly result from the discreteness of crystalline state. In Bloch's representation

$$|n\boldsymbol{k}\rangle = \psi_{n\boldsymbol{k}}(\boldsymbol{r}) = \frac{1}{\sqrt{N}} \mathrm{e}^{\mathrm{i}\boldsymbol{k}\boldsymbol{r}} u_{n\boldsymbol{k}}(\boldsymbol{r}) \ ,$$

the Green's function $G(n\boldsymbol{k}, n'\boldsymbol{k}', \omega) = \langle n, \boldsymbol{k}|G|n', \boldsymbol{k}'\rangle$ satisfies the following equation[8]:

$$[\omega - \varepsilon_n(\boldsymbol{k})]G(n\boldsymbol{k}, n'\boldsymbol{k}', \omega) - \sum_{j\boldsymbol{q}} V(n\boldsymbol{k}, j\boldsymbol{q})G(j\boldsymbol{q}, n'\boldsymbol{k}', \omega) = \delta_{nn'}\bar{\delta}(\boldsymbol{k} - \boldsymbol{k}'), \qquad (23)$$

where $\bar{\delta}(\boldsymbol{k}-\boldsymbol{k}')$ is the periodic extension of the delta function,

$$\bar{\delta}(\boldsymbol{k}-\boldsymbol{k}')=\frac{1}{N}\sum_{\boldsymbol{R}}\mathrm{e}^{\mathrm{i}(\boldsymbol{k}-\boldsymbol{k}')\cdot\boldsymbol{R}}=\sum_{\boldsymbol{K}}\delta(\boldsymbol{k}-\boldsymbol{k}'+\boldsymbol{K}),$$

$\varepsilon_n(\boldsymbol{k})$ is the band spectrum function, $\boldsymbol{K}$ is a reciprocal lattice vector, $N=N_{\parallel}N_z$ is the total number of the atoms, $V(n\boldsymbol{k},n'\boldsymbol{k}')$ is a matrix of the potential H_{I} and reads

$$\begin{aligned}V(n\boldsymbol{k},n'\boldsymbol{k}') &= \int \mathrm{d}\boldsymbol{r}\psi^{+}_{n\boldsymbol{k}}(\boldsymbol{r})H_{\mathrm{I}}\psi_{n'\boldsymbol{k}'}(\boldsymbol{r})=N_{\parallel}v(n\boldsymbol{k},n'\boldsymbol{k}')\bar{\delta}(\boldsymbol{k}_{\parallel}-\boldsymbol{k}'_{\parallel}),\\ v(n\boldsymbol{k},n'\boldsymbol{k}') &= \alpha_1\psi^{+}_{n\boldsymbol{k}}(0)\psi_{n'\boldsymbol{k}'}(0)+\alpha_2\psi^{+}_{n\boldsymbol{k}}(\boldsymbol{R}^0)\psi_{n'\boldsymbol{k}'}(\boldsymbol{R}^0)\,. \end{aligned}\tag{24}$$

After substituting $v(n\boldsymbol{k},n'\boldsymbol{k}')$, Eq.(23) can be written as

$$[\omega-\varepsilon_n(\boldsymbol{k})]G(n\boldsymbol{k},n'\boldsymbol{k}',\omega)-N_{\parallel}\sum_{jq_z}v(n\boldsymbol{k},j\boldsymbol{q})G(j\boldsymbol{q},n'\boldsymbol{k}',\omega)\big|_{\boldsymbol{q}=\boldsymbol{k}_{\parallel}+q_z\hat{\boldsymbol{z}}}=\delta_{nn'}\bar{\delta}(\boldsymbol{k}-\boldsymbol{k}')\,.\tag{25}$$

In a way similar to that used in sec.III, the solution of Green's function can be obtained

$$G(n\boldsymbol{k},n'\boldsymbol{k}',\omega)=G_0(n\boldsymbol{k},n'\boldsymbol{k}',\omega)+N_{\parallel}\frac{\psi^{+}_{n\boldsymbol{k}}(0)}{\omega-\varepsilon_{nk}}T_0+N_{\parallel}\frac{\psi^{+}_{n\boldsymbol{k}}(\boldsymbol{R}^0)}{\omega-\varepsilon_{nk}}T_z\,,\tag{26}$$

where G_0 is the Green's function of the unperturbed electron,

$$G_0=\frac{\delta_{nn'}\bar{\delta}(\boldsymbol{k}-\boldsymbol{k}')}{\omega-\varepsilon_n(\boldsymbol{k})}\,,\tag{27}$$

and

$$T_0=\frac{\nu^4}{\Delta}(p_{\circ}-\boldsymbol{p}\cdot\boldsymbol{\sigma})\left[\bar{Q}C_z+\left(\frac{\gamma}{\nu}-F-\frac{(\boldsymbol{\sigma}\cdot\boldsymbol{n})}{\nu}\right)C_0\right],$$

$$T_z=\frac{\nu^4}{\Delta}(p_{\circ}-\boldsymbol{p}^*\cdot\boldsymbol{\sigma})\left[QC_0+\left(\frac{\gamma}{\nu}-F-\frac{\sigma_z}{\nu}\right)C_z\right]\,,$$

with

$$C_0=\frac{\psi_{n'\boldsymbol{k}'}(0)}{\omega-\varepsilon_{n'}(\boldsymbol{k}')}\sum_{k_z}\bar{\delta}(\boldsymbol{k}-\boldsymbol{k}')\,,$$

$$C_z=\frac{\psi_{n'\boldsymbol{k}'}(\boldsymbol{R}^0)}{\omega-\varepsilon_{n'}(\boldsymbol{k}')}\sum_{k_z}\bar{\delta}(\boldsymbol{k}-\boldsymbol{k}')\,,$$

$$\Delta=1+\nu^4\left[\left(\frac{\gamma}{\nu}+F\right)^2-Q\bar{Q}\right]^2-2\nu^2\left[\left(\frac{\gamma}{\nu}+F\right)^2+Q\bar{Q}\cos\theta\right]\,.\tag{28}$$

In the above expression, p_0 and $\boldsymbol{p}$ are the same as that defined in sec.III for $F_1=F_2=F$, except that D^2 is replaced by $Q\bar{Q}$; F, Q and $\bar{Q}$ as functions of ω and $\mathbf{k}_{\parallel}$ are given, respectively, by

$$F=N_{\parallel}\sum_{nk_z}\frac{|\psi_{n\boldsymbol{k}}(0)|^2}{\omega-\varepsilon_n(\boldsymbol{k})}=-\mathrm{i}d_0\sum_n\frac{|u_{n\boldsymbol{k}}(0)|^2}{\hbar v_z^{(n)}}\,,\tag{29}$$

$$Q=N_{\parallel}\sum_{nk_z}\frac{\psi^{+}_{n\boldsymbol{k}}(0)\psi_{n\boldsymbol{k}}(\boldsymbol{R}^0)}{\omega-\varepsilon_n(\boldsymbol{k})}=-\mathrm{i}d_0\sum_n\frac{|u_{n\boldsymbol{k}}(0)|^2}{\hbar v_z^{(n)}}\mathrm{e}^{\mathrm{i}\boldsymbol{k}_{\parallel}\cdot\boldsymbol{R}^{\circ}_{\parallel}}\mathrm{e}^{\mathrm{i}k_zd}\,,\tag{30}$$

$$\bar{Q} = N_{\parallel} \sum_{nk_z} \frac{\psi_{n\boldsymbol{k}}(0)\psi^{+}_{n\boldsymbol{k}}(\boldsymbol{R}^0)}{\omega - \varepsilon_n(\boldsymbol{k})} = -\mathrm{i}d_0 \sum_n \frac{|u_{n\boldsymbol{k}}(0)|^2}{\hbar v_z^{(n)}} \mathrm{e}^{-\mathrm{i}\boldsymbol{k}_{\parallel}\cdot\boldsymbol{R}^0_{\parallel}} \mathrm{e}^{\mathrm{i}k_z d} \ , \tag{31}$$

where k_z, as a function of $\boldsymbol{k}_{\parallel}$ and ω, is determined by relation $\omega = \varepsilon_n(\boldsymbol{k})$, and $\hbar v_z^{(n)} = \frac{\partial \varepsilon_n(\boldsymbol{k})}{\partial k_z}$. It is apparent that the contribution to the functions F, Q and $\bar{Q}$ comes from the poles.

It is easy to obtain the following useful expression for the trace of Green's function:

$$\mathrm{Tr}G(\omega) = \sum_{n\boldsymbol{k}} G(n\boldsymbol{k}, n\boldsymbol{k}, \omega) = \mathrm{Tr}G_0(\omega) + N_z \sum_{\boldsymbol{k}_{\parallel}} \frac{\partial}{\partial \omega} \ln \Delta \ . \tag{32}$$

The DOS is given by

$$\rho(E) = \rho_0(E) - \frac{1}{\pi} \mathrm{Im} \sum_{\boldsymbol{k}_{\parallel}} \frac{\partial}{\partial \mathrm{E}} \ln \Delta|_{\eta \longrightarrow 0^+} \ , \tag{33}$$

and ECE

$$W = U_\theta - U_0 = -\frac{1}{\pi} \int_{-\infty}^{E_\mathrm{F}} \frac{\partial \Gamma}{\partial E}(E - E_\mathrm{F})\mathrm{d}E \ ,$$

$$\Gamma(E) = \mathrm{Im} \sum_{\boldsymbol{k}_{\parallel}} \ln \left(1 + \frac{4\nu^2 Q\bar{Q}}{\Delta_0} \sin^2\left(\frac{\theta}{2}\right)\right) \ , \tag{34}$$

where $\boldsymbol{k}_{\parallel}$ runs over the first Brillouin zone of a lattice plane which is parallel to the magnetic layer.

Equations (34) can be used to calculate ECE numerically. However, it is more meaningful to derive an analytical expression. For large distance, we can derive an asymptotic formula in the case of weak interaction. From the experience obtained in sec.III, we know that there may occur singularity in an individual term of expanding series; but the problem is not as serious as it looks; what we need to do is simply dismissing all the constant energy terms that appear in the final expression. So we can safely drop all constant terms in every step. Here, a new way which is equivalent to the stationary phase approximation is developed to obtain ECE in the single band regime.

Integrating by part, ECE given by Eq.(33) can be written as

$$W = \frac{\nu^2 \tau}{\pi^3} \sin^2\left(\frac{\theta}{2}\right) \mathrm{Im} \int_0^{k_z^m} \mathrm{d}k_z f(k_z) \mathrm{e}^{\mathrm{i}2k_z d} \ ,$$

$$f(k_z) = \int_{D(k_z)} \mathrm{d}\boldsymbol{k}_{\parallel} \frac{\hbar v_z F^2}{\Delta_0} \ ,$$

where only the leading term in the expanding series of Γ is kept, k_z^m is the maximum of the vertical wave vector, Im means imaginary part. Under the assumption that $\hbar v_z F^2/\Delta_0$ is a smooth function, it is apparent that f is a continuous function and after integration by part, W becomes

$$W = \frac{\nu^2 \tau}{\pi^3} \sin^2\left(\frac{\theta}{2}\right) \mathrm{Im} \int_0^{k_z^m} \frac{\mathrm{d}k_z}{2\mathrm{i}d} f'(k_z) \mathrm{e}^{\mathrm{i}2k_z d} \ ,$$

where prime stands for derivative, $f(k_z^m)=0$, which results from $D(k_z^m)=0$.

When the Fermi surface is given in the form $k_z = k_z(\boldsymbol{k}_\parallel)$, one can show that the derivative has a jump at the extreme points and is divergent logarithmically at the saddle points. In the neighborhood of a singular point $\boldsymbol{k}^{\rm c}$, the Fermi surface can be approximately described by

$$\begin{aligned} k_z &= k_z^{\rm c} + \lambda_x (k_x - k_x^{\rm c})^2 + \lambda_y (k_y - k_y^{\rm c})^2 \ , \\ \lambda_x &= \frac{1}{2}\frac{\partial^2 k_z}{\partial k_x^2}\bigg|_{\boldsymbol{k}^{\rm c}}, \qquad \lambda_y = \frac{1}{2}\frac{\partial^2 k_z}{\partial k_y^2}\bigg|_{\boldsymbol{k}^{\rm c}} \ . \end{aligned} \tag{35}$$

The λ_x and λ_y can be expressed by the effective mass and the group velocity

$$\lambda_x = -\frac{\hbar}{2m_x^* v_z} \ , \qquad \lambda_y = -\frac{\hbar}{2m_y^* v_z}.$$

To obtain Eq.(35), the coordinate system has been suitably chosen so that the cross derivative vanishes. We find that the first-order derivative $f'(k_z)$ is not a continuous function at an extreme point $\boldsymbol{k}^{\rm c}$

$$f'(k_z^{\rm c}+\epsilon) - f'(k_z^{\rm c}-\epsilon) = {\rm sgn}(\lambda_x)\frac{-\pi}{\sqrt{|\lambda_x\lambda_y|}}\frac{\hbar v_z F^2}{\Delta_0} \qquad \epsilon \to 0 \ , \tag{36}$$

where ${\rm sgn}(x)=1$ if $x>0$, and ${\rm sgn}(x)=-1$ if $x<0$; the second-order derivative $f''(k_z)$ has a pole at a saddle point $\boldsymbol{k}^{\rm c}$

$$f''(k_z) = \frac{1}{k_z - k_z^{\rm c}}\frac{1}{\sqrt{|\lambda_x\lambda_y|}}\frac{\hbar v_z F^2}{\Delta_0} \qquad k_z \to k_z^c \ . \tag{37}$$

We separate function f' into a regular part $f'_{\rm r}$, which is the same as f' except near the saddle point, and a singular part $f'_{\rm s}$, which vanishes far from saddle points and is divergent in a way similar to that of f' at the saddle points, $f' = f'_{\rm r} + f'_{\rm s}$. The integration of $f'_{\rm r}$ can be written as

$$\begin{aligned} \int_0^{k_z^m} {\rm d}k_z f_r'(k_z){\rm e}^{{\rm i}2k_z d} &= \int_0^{k_z^{\rm c_1}-\epsilon} {\rm d}k_z f_r'(k_z){\rm e}^{{\rm i}2k_z d} + \int_{k_z^{\rm c_1}+\epsilon}^{k_z^{\rm c_2}-\epsilon} {\rm d}k_z f_r'(k_z){\rm e}^{{\rm i}2k_z d} \\ &\quad + \cdots + \int_{k_z^{\rm cr}+\epsilon}^{k_z^m} {\rm d}k_z f_{\rm r}'(k_z){\rm e}^{{\rm i}2k_z d} \\ &= -\frac{1}{2{\rm i}d}\sum_{\boldsymbol{k}^{\rm c}} [f(k_z^{\rm c}+\epsilon) - (f(k_z^{\rm c}-\epsilon)]{\rm e}^{{\rm i}2k_z^{\rm c} d} \ . \end{aligned}$$

Since $f'_{\rm s}$ is assumed to be a highly localized function, we can extend the integration interval to the whole axis

$$\begin{aligned} \int_0^{k_z^m} {\rm d}k_z f_{\rm s}'(k_z){\rm e}^{{\rm i}2k_z d} &= \int_{-\infty}^{\infty} {\rm d}k_z f_{\rm s}'(k_z){\rm e}^{{\rm i}2k_z d} = -\frac{1}{2{\rm i}d}\int_{\infty}^{\infty} {\rm d}k_z f_{\rm s}''(k_z){\rm e}^{{\rm i}2k_z d} \\ &= -\frac{{\rm i}\pi}{2{\rm i}d}\sum_{\boldsymbol{k}^{\rm c}} {\rm Res}(f_{\rm s}''){\rm e}^{{\rm i}2k_z^{\rm c} d} \ , \end{aligned}$$

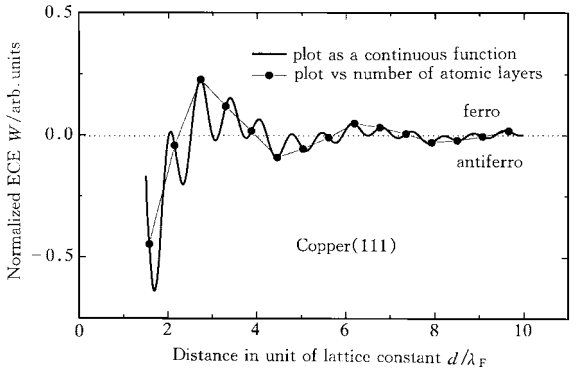

Fig.5. Calculated ECE for two magnetic layers in metal copper (111).

Summarizing all the above results, we finally obtain

$$W = \frac{(JsS)^2}{2\pi^2\hbar^2(1-\gamma^2)\tilde{d}^2}\sin^2\left(\frac{\theta}{2}\right)\sum_{\boldsymbol{k}^c}\sqrt{|m_x^* m_y^*|}\,|u_{\boldsymbol{k}}(0)|^4\sin(2k_z d+\phi)\,|_{\boldsymbol{k}^c}\quad , \tag{38}$$

where $\tilde{d} = d/d_0$, $\phi = 0$ for maximum, $\phi = \pi/2$ for saddle, $\phi = \pi$ for minimum. Equation (38) has been used to evaluate ECE for the case with magnetic layers embedded in copper (see Fig.5). The long period is really about 6 monolayers, which is in agreement with experimental result. Similar result had been first given by Bruno *et al.* in a different way.[3] For noble metals, as shown in Ref [3], the periods observed in experiments can be predicted correctly by using Eq.(38).

REFERENCES

[1] F. Grunberg, R. Schreiber, Y. Pang, M. N. Brodsky and H. Sowers, *Phys. Rev. Lett.*, **57** (1986), 2442.
[2] S. S. P. Parkin, N. More and K. P. Roche, *Phys. Rev. Lett.*, **64** (1990), 2304; S. S. P. Parkin, R. Bhadra and K. P. Roche, *Phys. Rev. Lett.*, **66** (1991), 2152.
[3] P. Bruno and C. Chappert, *Phys. Rev. Lett.*, **67** (1991), 1602; *Phys. Rev.*, **B46** (1992), 261.
[4] D. M. Edwards, J. Mathon, P. B. Muniz and M. S. Phan, *Phys. Rev. Lett.*, **67** (1991), 493.
[5] M. D. Stiles, *Phys. Rev.*, **B48** (1993), 7238.
[6] J. Barnas, *J. Magn. Magn. Mater.*, **111** (1992), L215.
[7] R. P. Erickson, Kristl B. Hathaway and James R. Cullen, *Phys. Rev.*, **B47** (1993), 2626.
[8] Wang Shaofeng, Wang Zhongcheng, Zou Shichang, *Phys. Rev.*, **B53** (1996), 12225.
[9] J. S. Helman and W. Baltensperger, *Phys. Rev.*, **B53** (1996), 275.
[10] M. R. Halse, *Philos. Trans. R. Soc. London*, **256** (1969), 507.
[11] C. Kittel, in Solid State Physics, edited by F. Seitz, D. Turnbull and H. Ehrenreich (Academic, New York, 1968), Vol.22, p.11.
[12] Y. Yafet, *Phys. Rev.*, **B36** (1987), 3948.